

# Determination of X-Ray Transient Source Positions By Bayesian Analysis of Coded Aperture Data

Carlo Graziani,<sup>1</sup> Donald Q. Lamb,<sup>1</sup> and Raphael Slawinski<sup>2</sup>

<sup>1</sup> Dept. of Astronomy & Astrophysics, University of Chicago

<sup>2</sup> Dept. of Geophysics, University of Calgary

*E-mail: c-graziani@uchicago.edu*

## ABSTRACT

We present a new method of transient point source deconvolution for coded-aperture X-Ray detectors. Our method is based upon the calculation of the likelihood function and its interpretation as a probability density for the transient source position by an application of Bayes' Theorem. The method obtains point estimates of source positions by finding the maximum of this probability density, and interval estimates of prescribed probability by choosing suitable contours of constant probability density. We give the results of simulations that we performed to test the method. We also derive approximate analytic expressions for the predicted performance of the method. These estimates underline the intuitively plausible properties of the method and provide a sound quantitative basis for the design of coded-aperture systems.

KEY WORDS: techniques: image processing — gamma rays: bursts

## 1. Introduction

The nature and origin of gamma-ray bursts is a mystery of twenty-five years' standing. The identification of counterparts at other wavelengths is the "Holy Grail" of GRB studies, since it is widely believed that this is the most likely approach to crack the mystery. The consensus is that the next step in GRB instrumentation is to obtain few-arc-minute or better scale GRB sky locations in bulk, possibly in real time. This can be accomplished effectively by means of a triggered coded-aperture X-ray instrument such as the one planned for HETE (Ricker 1997).

Several processing methods for coded-aperture data have been proposed, including cross correlation (Fenimore 1978), least-squares fitting (Doty 1978), and Maximum Entropy (Sims et al. 1980, Willingdale et al. 1984). Skinner and Nottingham (1993) have described a maximum-likelihood fitting technique. We present here a Bayesian scheme for analyzing coded-aperture data from such transient events. The method is based on the calculation of the joint likelihood function for two stretches of data: the stretch covering the transient event itself, and a stretch before and/or afterwards, which provides information about the background. We interpret the likelihood thus obtained as a posterior probability density for the transient event location by an application of Bayes' Theorem (for a lucid discussion of astrophysical applications of Bayesian inference, see Loredó 1992).

This probability density has several uses. Its max-

imum provides a point estimate for the location of the transient source. We can also use it to obtain a 68% credible region for the location of the source. Finally, we can use semi-analytical approximations to this probability distribution to predict the performance of the method, and to state detector design criteria useful for optimizing the angular resolution of the instrument.

## 2. The Posterior Probability Density

We begin by exhibiting the posterior probability density for the transient position. The discussion in this section is rather similar to the discussion in Loredó (1992) of Bayesian inference of a Poisson mean, which may usefully be read for comparison.

We assume that a (one- or two-dimensional) coded-aperture instrument is illuminated by a transient source. The instrument consists of a position-sensitive detector with  $N_{\text{det}}$  position bins, beneath a coded-aperture mask. We denote the "background" counts observed during a period  $T_{\text{bk}}$  prior to the onset of the transient event by  $\vec{b}$ , where the  $i$ th component of  $\vec{b}$  is  $b_i$ ,  $i = 1, \dots, N_{\text{det}}$ . We denote by  $\vec{g}$  the gross counts observed during a time  $T_{\text{burst}}$  while the transient event was occurring. The background  $\vec{b}$  includes the diffuse X-ray background and the particle background, as well as any steady point sources in the field of view. The gross counts  $\vec{g}$  reflect the shadow pattern of the coded-aperture mask on the detector as cast by the illumination of the transient source, super-

posed upon the previously measured steady background.

We denote by  $\Omega \equiv (\theta, \phi)$  the direction towards the transient source. We denote the characteristic shadow pattern of the mask illuminated by a source in the direction  $\Omega$  by  $\bar{\tau}(\Omega)$ , where we adopt the normalization  $\sum_{i=1}^{N_{\text{det}}} \tau_i = 1$ . We further denote the expected number of total counts due to the transient by  $\omega$ , so that the expected number of counts in the  $i$ th bin due to the transient source is  $\omega \tau_i$ .

If we assume prior probability densities that are uniform in the background Poisson rates, in  $d\omega$ , and in  $d\Omega = d\cos\theta d\phi$ , and integrate over the unknown background rates and over  $\omega$ , we obtain the following expression for the desired posterior probability density:

$$P(\Omega|\vec{g}, \vec{b}, I) = \kappa \int_0^\infty d\omega e^{-\omega} \times \prod_{i=1}^{N_{\text{det}}} \left\{ \sum_{s_i=0}^{g_i} \frac{(s_i + b_i)!}{b_i! s_i! (g_i - s_i)!} \frac{(\omega \tau_i)^{g_i - s_i} (T_{\text{burst}}/T_{\text{bk}})^{s_i}}{(1 + T_{\text{burst}}/T_{\text{bk}})^{s_i + b_i + 1}} \right\}, \quad (1)$$

where  $\kappa$  is a normalization constant. If instead of integrating over the unknown background rates, we assume that  $T_{\text{bk}}$  is sufficiently long that the observation of the  $b_i$  determines the rates accurately, we find instead the simpler approximate formula

$$P(\Omega|\vec{g}, \vec{b}, I) \approx \kappa \int_0^\infty d\omega e^{-\omega} \times \prod_{i=1}^{N_{\text{det}}} [\omega \tau_i + (T_{\text{burst}}/T_{\text{bk}}) b_i]^{g_i}. \quad (2)$$

In these equations, the  $\tau_i(\Omega)$  represent our understanding of the detector response. We may estimate them by simple ray-tracing of the mask pattern onto the detector, or they may be determined by Monte Carlo simulations that account for physical effects (Compton scattering by various elements of the spacecraft and instrument, finite detector resolution, blurring due to the finite thickness of the coded aperture mask, etc.) as well as purely geometric effects.

The procedure we have used to arrive at equations (1) and (2) may be described as a joint fit of the background and event data, followed by an integration over the unknown background Poisson means, which are uninteresting parameters. While this procedure may seem unfamiliar, it is merely the Poisson version of the familiar Gaussian technique of background subtraction. In fact, if the data consisted of Gaussian rather than Poisson deviates, with the likelihood proportional to  $e^{-\chi^2/2}$ , we would be led directly to the usual formula for the  $\chi^2$  of a background-subtracted signal. To press the analogy further, the passage from eq. (1) to eq. (2) is analogous to the neglect in Gaussian theory of the contribution to

the variance due to the uncertainty in the measurement of the background.

Thus, this method is related to the “ $\chi^2$ -fitting approach” to coded-aperture data analysis (Doty 1978) in the sense that, to within an additive constant,  $\chi^2$  is proportional to the log likelihood in the Gaussian limit of many counts. In fact, the likelihood method constitutes a generalization of the  $\chi^2$  method which is robust even in the limit of low signal-to-noise.

We may use eqs. (1) or (2) (depending on the background rate and on  $T_{\text{bk}}$ ) in two ways. We may estimate the location of the transient on the sky by maximizing the probability density with respect to  $\Omega$ , obtaining in effect the maximum likelihood estimate of the location. We may also use the probability density to obtain, say, a 68% probability Bayesian confidence region for the location of the transient. We choose a grid of points that is *uniform in an equal-area projection of the field of view* near the estimated location of the transient, and calculate the probability density at each point of the grid. We choose  $\kappa$  so that the sum over the grid is normalized to 1, and find the value of the probability density such that the sum of the probabilities of grid points that exceed this value is 68%.

### 3. Simulations

#### 3.1. Signal-to-Noise Study

For illustrative and pedagogical purposes, we have simulated a highly idealized coded-aperture instrument patterned after the HETE WXM. This detector consists of two crossed, one-dimensional position-sensitive proportional counters (PSPCs), one each in the  $x$  and  $y$  directions. The length of a PSPC bin is 0.1 cm. At a distance 18.73 cm above each PSPC is a one-dimensional random array coded-aperture mask. The length of a mask element is 0.2 cm. Note that the “natural” resolution unit for this ideal detector is the ratio of the bin size to the height of the mask above the PSPC, i.e.  $\sim 18'$ .

We model the  $\tau_i$  using only geometric shadowing by the coded aperture mask and the detector walls, and projection effects; no physical effects (such as the ones alluded to in the previous section) are included. The encoded images obtained during the intervals  $T_{\text{burst}}$  and  $T_{\text{bk}}$  are thus degraded by Poisson noise only.

Figures 1 and 2 show the result of analyzing simulations at  $(\theta = 30^\circ, \phi = 45^\circ)$ , for signal-to-noise ratios (S/N) of 10, 5, 3, and 1. The probability density was calculated using eq. (1). The solid, dashed, and dotted contours represent 68.3%, 95.5%, and 99.7% Bayesian confidence regions, respectively.

The figures show that for high S/N, the angular resolution can be considerably better than the “natural” resolution, while the instrument’s angular resolving power starts to “melt down” at about S/N=3. Note that the

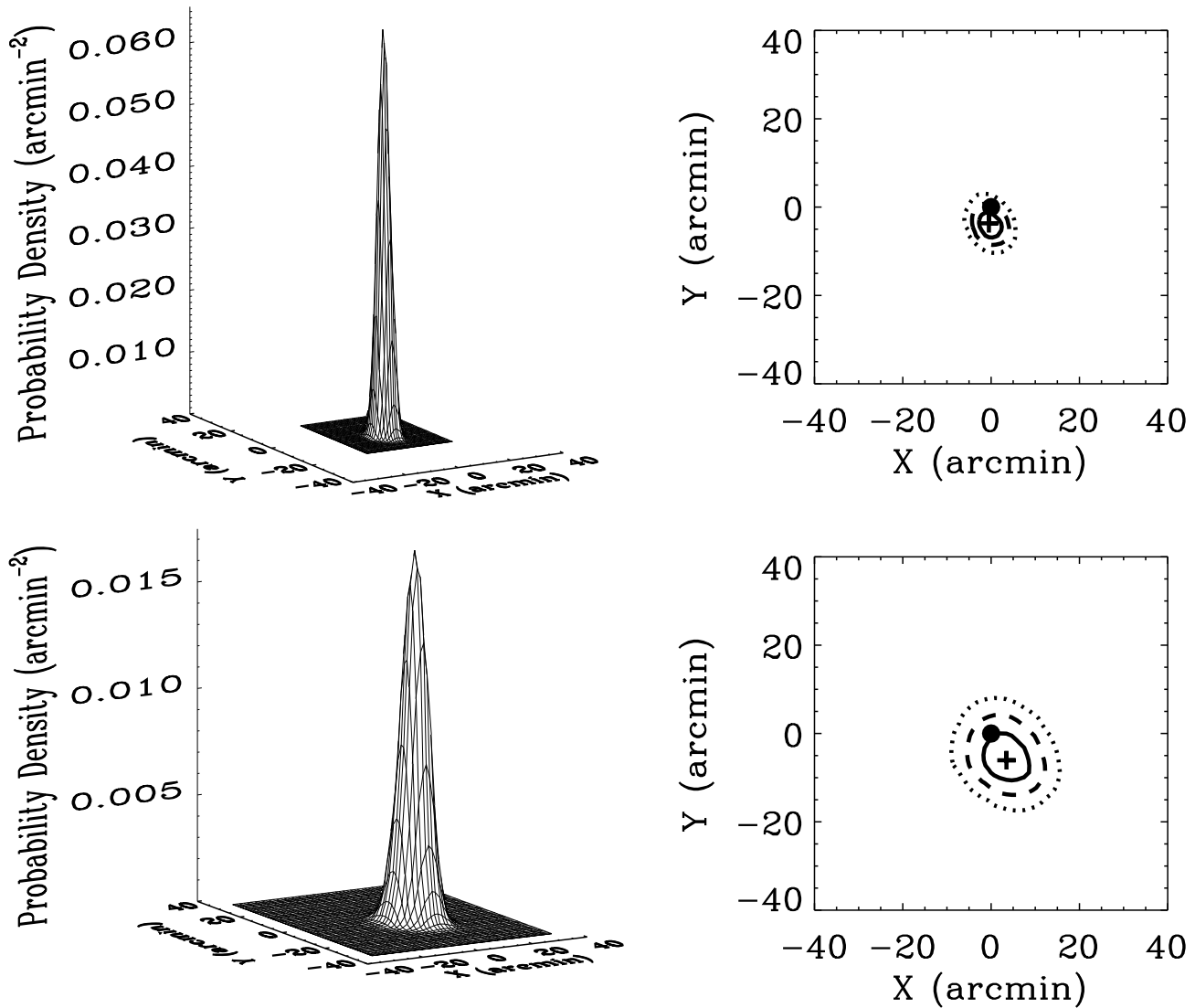


Fig. 1. Analysis of simulated data assuming a transient event from the direction  $\theta = 30^\circ$ ,  $\phi = 45^\circ$ . The plots on the left show the probability density, while the plots on the right show the 1-, 2-, and 3- $\sigma$  contours for the transient location, as well as the true location (dot) and the maximum-likelihood point (cross). The  $X$  and  $Y$  axes are cartesian coordinates in an equal-area projection, shifted so as to place the true event location at the origin. Top panel:  $S/N=10$ . Bottom panel:  $S/N=5$ .

$S/N$  is for the entire event, not just for the trigger interval, so that even events discovered near or below a 3- $\sigma$  trigger threshold may be successfully located.

### 3.2. Contour Calibration Study

By construction, the contours chosen by this procedure have the following property: If in simulations we choose locations from a distribution of locations that is uniform in the FOV, and for each location we simulate data and calculate a credible region, in the long run the credible region will bracket the “true” location of the simulated transient 68% of the time.

We tested this property by simulating many transients

events. The position of each event was drawn randomly from a uniform distribution on the sky, limited to an angle from the detector normal of less than  $20^\circ$ . Each transient event was superposed on a background of 1 count  $s^{-1} \text{ bin}^{-1}$ , and was assigned  $S/N=3$  for the entire detector. The background stretch lasted 100 sec for each event.

Note that from the plots in Figure 2,  $S/N=3$  is about where the linearity of the model in the position parameters begins to break down, so that the posterior density looks significantly non-Gaussian. This is the regime where we would expect to lose faith in the correctness of

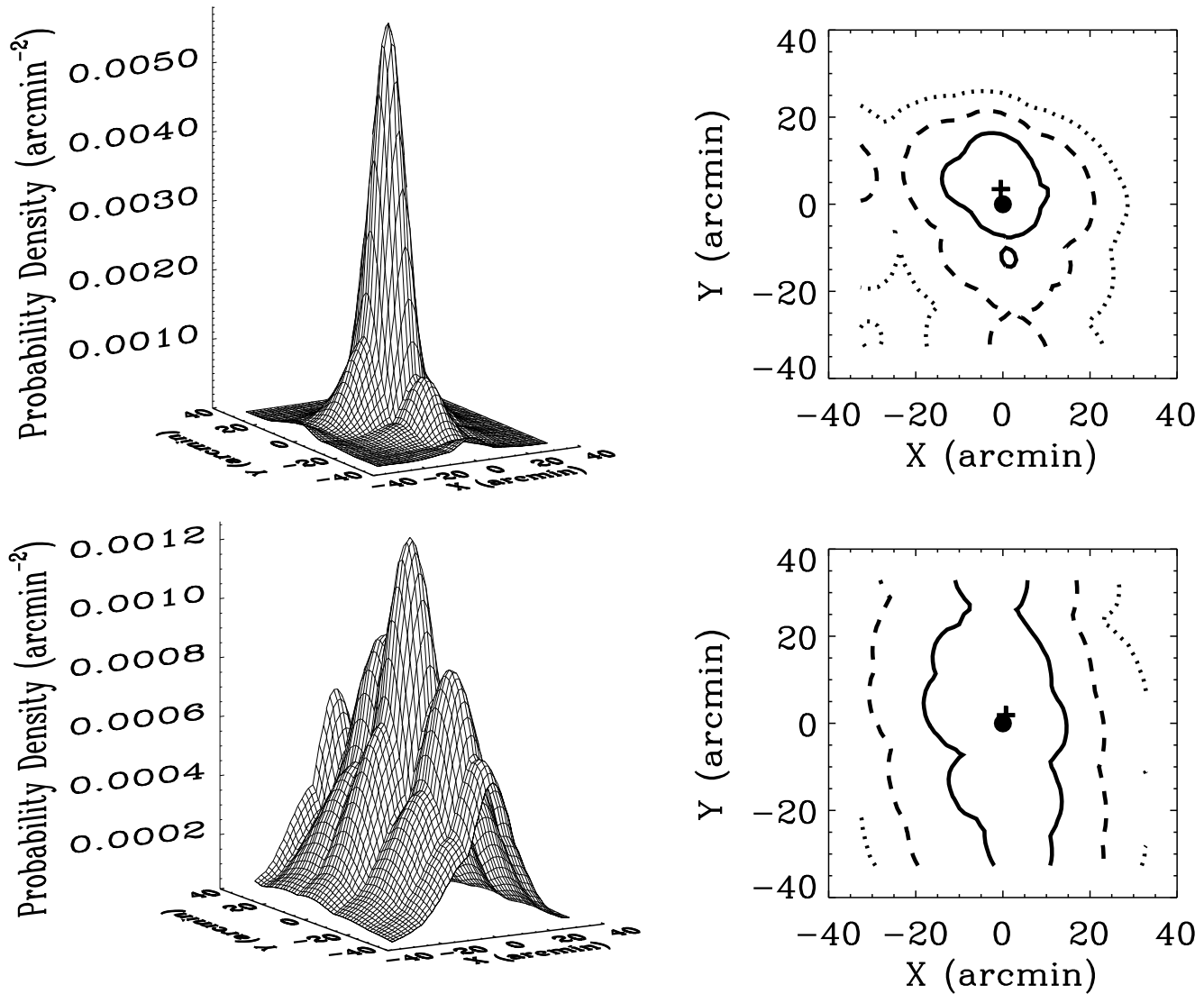


Fig. 2. Analysis of simulated data assuming a transient event from the direction  $\theta = 30^\circ$ ,  $\phi = 45^\circ$ . The plots on the left show the probability density, while the plots on the right show the 1-, 2-, and 3- $\sigma$  contours for the transient location, as well as the true location (dot) and the maximum-likelihood point (cross). The  $X$  and  $Y$  axes are cartesian coordinates in an equal-area projection, shifted so as to place the true event location at the origin. Top panel:  $S/N=10$ . Bottom panel:  $S/N=3$ .

the calibration of contours obtained using the  $\chi^2$  procedure of Lampton, Margon, and Bowyer (1976).

We simulated 1000 events, in each case calculating the 68.3%, 95.5%, and 99.7% contours and recording whether the contours included the “true” position. The number of such “hits” is binomially distributed, so that if the contours of probability value  $p$  bracket the true position  $b$  times in  $n$  attempts, we may use as a statistical measure of the plausibility of this result the cumulative distribution function  $Q(b) \equiv \sum_{j=0}^b n!/j!(n-j)! \times p^j(1-p)^{n-j}$ .  $Q(b)$  should be approximately uniformly distributed in the interval  $[0, 1]$ , so the result will

be plausible unless  $Q(b)$  is found to be excessively close to either 0 or 1.

Out of 1000 simulated events, we found that the 68.3% contour bracketed the true event position 675 times ( $Q = 0.30$ ), the 95.5% contour did so 956 times ( $Q = 0.58$ ), and the 99.7% contour did so 996 times ( $Q = 0.35$ ). Thus the contours produced by the method appear to be well-calibrated (as expected), in the sense that the long-term frequency with which the contours bracket the true positions are indeed consistent with their nominal probability values.

#### 4. Semi-Analytic Resolution Estimate

We now introduce some analytical approximations in order to develop some intuition regarding the method described in the previous section. These approximate estimates are helpful for optimization of detector parameters, and also allow us to verify that our simulations of the method, described in the previous section, behave as expected.

For concreteness, we specialize our analysis to coded-aperture systems similar to the HETE WXM. This is not a very serious restriction, since other coded-aperture detectors (such as the ASM on the *Rossi* X-Ray Timing Explorer) have fairly similar designs. In any event, generalization to other types of coded-aperture detectors is straightforward.

The HETE WXM consists of two crossed, one-dimensional PSPCs, one each in the  $x$  and  $y$  directions. Above each PSPC is a one-dimensional coded-aperture random array mask.

Let the PSPC bin the data in  $N_{\text{det}}$  position bins of length  $\Delta$ , and let  $N_{\text{det}} \times \Delta \equiv L_{\text{det}}$ . Also, assume that the mask consists of  $N_{\text{mask}}$  adjacent elements of length  $l$ , each of which may be open or closed, and define  $N_{\text{mask}} \times l \equiv L_{\text{mask}}$ . For HETE,  $L_{\text{mask}} > L_{\text{det}}$ , and  $l > \Delta$ , and we assume this is so in the present analysis. Let  $h$  be the height of the mask above the PSPC. We further define the mask's open fraction  $t$ , which is such that  $tN_{\text{mask}}$  is equal to the number of open mask elements. Finally, we assume that the spatial resolution of the PSPC is described by a smearing function  $g_a(x - y)$ , which is the probability that a photon deposited at a position  $y$  on the PSPC is recorded with a position  $x$  in range  $dx$ . It is assumed to have a width  $a$ . Finally we define  $\psi$  as the expected number of transient source counts per bin assuming a  $t = 1$  mask, and  $\eta$  as the expected number of background counts per bin assuming a  $t = 1$  mask.

Assuming the direction of the transient is not too far from the detector normal, we may evaluate the detector resolution by estimating the width of the central peak of the probability density, in the form given in eq. (2). The angular variation of the probability density may be traced to the variation with the assumed transient source position of the shadows of mask element edges on the detector. The angular resolution thus increases with increasing number of edge shadows on the detector, as well as with increasing sharpness of the edge shadows. Guided by this observation we have shown that the detector angular resolution  $\delta\theta$  is approximately given by

$$\delta\theta \approx S_a^{-1} \left\{ 2F(\theta) \left( \frac{h}{\Delta} \right)^2 \left( \frac{L_{\text{det}}}{l} \right) \left( \frac{\psi^2}{\eta} \right) \times \frac{1-t}{1 + \frac{\psi}{2\eta} \frac{1}{t}} \right\}^{-\frac{1}{2}}, \quad (3)$$

where

$$S_a \equiv \int_{-\Delta/2}^{+\Delta/2} dx g_a(x), \quad (4)$$

and where  $F(\theta)$  is the fraction of the detector that is not shadowed by the detector walls for a transient source at  $\theta$ . For the 1000 simulations discussed in the previous section, we find that this expression, translated into a confidence region, is in good agreement (10%-20%) with the actual confidence region sizes.

Equation (3) may be readily interpreted as follows:

As is intuitively reasonable,  $\delta\theta \propto \Delta/h$ . Thus the angular resolution is naturally expressed in units of the angle subtended at the mask by a detector bin size. It follows that it is desirable to design the coded-aperture system with as small a  $\Delta/h$  as possible. Of course, increasing  $h$  reduces the field of view and increases the penalty imposed by the factor  $F(\theta)^{-1/2}$  for off-axis events.

Furthermore,  $\delta\theta \propto (L_{\text{det}}/l)^{-1/2}$ , which accounts for the “tiling” of the detector by the mask elements — this factor in effect counts the number of mask element edges that cast their shadows on the detector. Clearly, it places a premium on as small an  $l$  as possible, that is,  $l = \Delta$ . Thus it appears that “oversampling” of the mask by the detector is not beneficial.

When  $\psi \gg \eta$ , we have  $\delta\theta \propto 1/\psi^{1/2}$ , while when  $\psi \ll \eta$ , we have  $\delta\theta \propto \eta^{1/2}/\psi$ . Thus in either case,  $\delta\theta \propto 1/\text{SNR}$ .

The dependence of  $\delta\theta$  on  $t$  is relatively simple. There is an “optimal”  $t_{\text{opt}}$  that minimizes  $\delta\theta$ , given by

$$t_{\text{opt}} = -\frac{\psi}{2\eta} + \frac{1}{2} \left[ \left( \frac{\psi}{\eta} \right)^2 + 2\frac{\psi}{\eta} \right]^{\frac{1}{2}}. \quad (5)$$

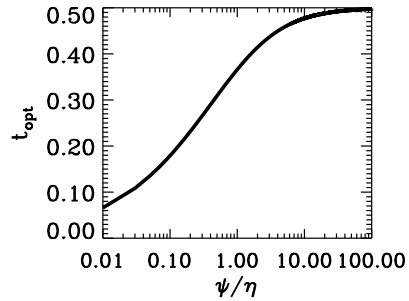


Fig. 4. Optimum transmission fraction as a function of signal-to-background.

The behavior of  $t_{\text{opt}}$  as a function of  $\psi/\eta$  is shown in Figure 4. The form of  $t_{\text{opt}}$  is different from the one found by previous authors (Fenimore 1978, in’t Zand, Heise, & Jager 1994), although the functional dependence is still

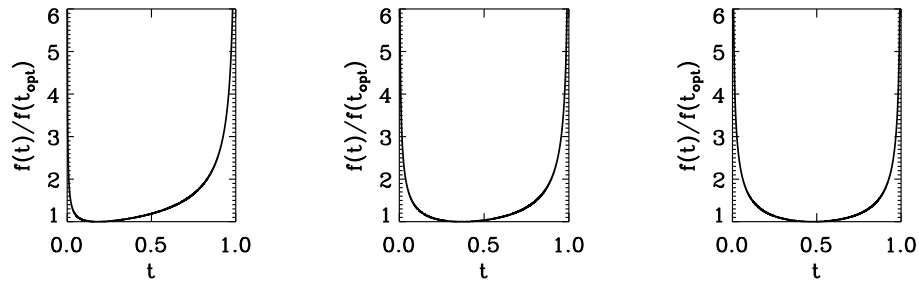


Fig. 3. Angular resolution as a function of transmission fraction  $t$ , for  $\psi/\eta=0.1, 1$ , and  $10$ . The function  $f(t)$  is given by  $[(1+\psi/2\eta t)/(1-t)]^{1/2}$ . The quantity  $t_{\text{opt}}$  is the optimum transmission fraction for the given signal-to-background.

on the signal-to-background. The difference is ascribable to the difference in the quantities optimized: the previous work optimized the signal-to-noise in the resolution element corresponding to the source, whereas in this work we optimize the angular resolution directly.

Figure 3 shows the  $t$  dependence of  $\delta\theta$  for signal-to-background ratios of  $0.1, 1$ , and  $10$ . It is clear from this figure that precisely optimizing  $t$  is not critical. The  $t$ -dependence of the resolution is a very forgiving function, with relatively large differences from  $t_{\text{opt}}$  costing relatively little in resolution.

Finally, the factor  $S_a$  accounts for the smearing by the detector of the otherwise perfectly sharp shadows of the mask element edges. It is the “migration” with assumed source position of these shadows across the PSPC bins that gives the probability density its sensitivity to the transient location, and which makes possible resolutions  $\delta\theta < \Delta/h$ . Naturally, the linear resolution of the PSPC degrades the angular resolution of the instrument, by a factor given by  $S_a$ . Note that  $S_a \rightarrow 1$  as  $a \rightarrow 0$ .

## 5. Conclusions

The likelihood function approach to coded-aperture data analysis is a very powerful method that makes maximal use of the information borne by the data. The method produces not only point estimates of source position, but also credible regions that are well-calibrated in the sense that in the long run, a 68% region brackets the true location in 68% of simulations. This remains the case even in the low signal-to-noise case, where linear methods lose their statistical reliability. The method can produce angular resolution in excess of the “natural” resolution of the detector, for high signal-to-noise ratios.

In addition, a semi-analytic estimate of the angular resolution gives a result that is intuitively plausible and provides useful guidance for coded-aperture instrument design. In particular it provides a novel criterion for assessing the impact of the choice of transmission fraction of the coded-aperture mask, and indicates that it is

not beneficial to design a position-sensitive detector that “oversamples” the mask pattern.

## Acknowledgements

We thank Tom Loredo for clarifying the calibration properties of Bayesian credible regions, and John Doty for pointing out an error in an early version of the paper.

## References

- Doty J. P. 1978, in *X-Ray Instrumentation in Astronomy II*, ed. L. Golub, Proc SPIE, 982, 164
- Fenimore E. E. 1978, *Appl. Opt.*, 17, 3562
- in’t Zand J. J. M., Heise J., and Jager, R., 1994, *A&A*, 288, 665
- Lampton M., Margon B., and Bowyer S., 1976, *ApJ*, 208, 177
- Loredo T. J. 1992, in *Statistical Challenges in Modern Astronomy*, ed. E. Feigelson and G. Babu (New York: Springer-Verlag), p. 275
- Ricker G. R. 1997, these proceedings
- Sims M., Turner M.J.L., and Willingale R. 1980, *Space Sci. Instrum.*, 5, 109
- Skinner G. K., and Nottingham M. R. 1993, *Nucl. Instrum. Methods Phys. Res.*, A333, 540
- Willingale R., Sims M., and Turner M.J.L. 1984, *Nucl. Instrum. Methods Phys. Res.*, 221, 60